Conclusion

Integral equations relating the source function, emissive power, and heat source for gas, and leaving intensity, emissive power, and heat flux for surfaces are developed for anisotropically scattering media. When the gas scatters isotropically and surfaces are diffuse, these equations are reduced to the radiosity formulations given by Hottel and Sarofim.[3] The source function distribution in gas and leaving intensity distribution on surface can be obtained by solving the discrete form of these equations. The present method can be used for radiative heat transfer analysis of isotropic or anisotropic scattering media, and the results are in good agreement with those of the existing methods. The computational time is reasonably low for isotropically scattering problems. For anisotropically scattering cases, however, the computational time can become quite high.

In the zonal method, the radiosities are net radiative energy leaving finite gas volumes and finite surface areas. To calculate these radiosites, direct exchange areas between finite volume and surfaces must be evaluated. Substantial computational efforts are usually used to evaluate multiple integrations of the exchange areas. In the present approach, however, the exchange factors between nodal points are used. Consequently, substantial computational time can be saved by avoiding multiple integrations in the exchange factor computation without sacrificing the accuracy.

Most recently, Saltiel and Naraghi[9-10] have demonstrated that by using a rectangular (midpoint) numerical integration method, the DEF method can be applied to geometrically complex problems. Because the exchange factors and numerical discretization method used in the present approach is the same as DEF method, the present method can also be easily applied to geometrically complex problems.

References

[1]Huan, J., and Naraghi, M. H. N., "Analysis of Radiative Heat Transfer in Three Dimensional Absorbing, Emitting, and Scattering Media—A Source Function Approach," *Radiation Heat Transfer*, edited by S. T. Thynell and J. R. Mahan, American Society of Mechanical Engineers Publication HTD-Vol. 154, Presented at the American Society of Mechanical Engineers Winter Annual Meeting, Dallas, TX, Nov. 25–30, 1990, pp. 59–66.

[2]Naraghi, M. H. N., Chung, B. T. F., and Litkouhi, B., "A Continuous Exchange Factor Method for Radiative Exchange in Enclosures with Participating Media," *Journal of Heat Transfer*, Vol. 110, No. 2, 1988, pp. 456–462.

[3]Hottel, H. C., and Sarofim, A. F., *Radiative Transfer*, McGraw-Hill, New York, 1967.

[4]Larsen, M. E., "Exchange Factor Method and Alternative Zonal Formulation for Analysis of Radiating Enclosures Containing Participating Media," Ph.D. Thesis, Univ. of Texas, Austin, TX, 1983.

[5]Naraghi, M. H. N., and Litkouhi, B., "Discrete Exchange Factor Solution of Radiative Heat Transfer in Three-dimensional Enclosures," *Heat Transfer Phenomena in Radiation, Conduction, and Fire*, edited by R. K. Shah, American Society of Mechanical Engineers Publication HTD-Vol. 106, Presented at the National Heat Transfer Conference, Philadelphia, PA, Aug. 6–9, 1989, pp. 221–229.

[6]Fiveland, W. A., "Three-Dimensional Radiative Heat Transfer Solution by the Discrete-Ordinate Method," *Journal of Thermophysics and Heat Transfer*. Vol. 2, No. 4, 1988, pp. 309–316.

[7]Naraghi, M. H. N., and Huan, J., "An N-Bounce Method for Analysis of Radiative Transfer in Enclosures with Anisotropically Scattering Media," *Journal of Heat Transfer*, Vol. 113, No. 3, 1990, pp. 774–777.

[8]Mengüç, M., and Viskanta, R., "Radiative Transfer in Three-Dimensional Rectangular Enclosures, *Journal of Quantitative Spectroscopy and Radiative Heat Transfer*, Vol. 33, 1985, pp. 533–549.

[9]Saltiel, C., and Naraghi, M. H. N., "Analysis of Radiative Heat Transfer in Participating Media Using Arbitrary Nodal Distribution," *Numerical Heat Transfer*, Vol. 17, 1990, pp. 227–243.

[10]Saltiel, C., and Naraghi, M. H. N., "Combined-Mode Heat Transfer in Radiatively Participating Media Using the Discrete Exchange Factor Method with Finite Elements," Heat Transfer 1990, Hemisphere Publishing Corp., Vol. 6, pp. 391–396.

Transient Heat-Pipe Modeling: A Quasisteady, Incompressible Vapor Model

W. Jerry Bowman*
Air Force Institute of Technology, Wright-Patterson Air Force Base, Ohio 45433
and
Robert C. Winn† and Harold L. Martin‡
U. S. Air Force Academy, Colorado Springs, Colorado 80840

Introduction

MANY approaches have been taken regarding the numerical modeling of transient heat-pipe vapor phenomena. The most complicated models assume the vapor flow is two-dimensional, compressible, and unsteady.[1-4] These models are useful in understanding the detailed physics of vapor transients; unfortunately, they require the use of large amounts of computer time. Simpler approaches that model the flow as one-dimensional but still compressible and unsteady have been shown to save great amounts of computer time while still adequately modeling the heat-pipe vapor behavior.[5-8] Methods of accelerating the solution process by using local time-stepping techniques have proved effective in saving computer time when the one-dimensional models are used.[9] All of the models mentioned above have assumed the vapor behaves like an ideal gas. This assumption has often been questioned, but an alternative approach has never been presented.

For the vapor model described in this paper, the vapor flow is assumed to be one-dimensional, compressible in time, incompressible in space, and quasisteady. The vapor is not assumed to be an ideal gas, but is assumed to be a saturated vapor. By assuming the flow is incompressible in the spatial coordinate, and the vapor is a saturated vapor, the vapor modeling problem is greatly simplified. This means both the vapor density and temperature are spatially constant and dependent. As shown below, the transient is modeled by keeping track of the mass and energy leaving and entering the vapor space. At any time during the transient, the vapor velocity distribution and pressure distribution along the heat-pipe can be found, but unlike earlier models, they aren't required as part of the solution process. This saves a great deal of computer time.

Numerical Model

The Wall Model

The transient energy conduction in the heat-pipe wall is modeled by solving the two-dimensional, constant properties, transient, heat diffusion equation. For this work, an explicit, finite difference solution technique is used[10]; however, other methods should work equally well. The temperature of the heat-pipe's external evaporator surface is specified as a boundary condition. A zero temperature gradient is specified as the boundary condition along the external surface of the adiabatic section. A convection boundary condition is used on the external condenser surface. The condenser external environment temperature is specified as part of that boundary condition.

Received March 20, 1991; revision received Sept. 1, 1991; accepted for publication Oct. 5, 1991. This paper is declared a work of the U.S. Government and is not subject to copyright protection in the United States.

*Associate Professor of Aeronautics. Member AIAA.
†Professor of Aeronautics. Associate Fellow AIAA.
‡Assistant Professor of Aeronautics.

Along the inside surface of the heat-pipe (wall/vapor interface), an evaporation/condensation boundary condition is used. The conduction energy flux leaving the internal wall surface is set equal to the energy convected to the vapor. The energy convected to the vapor is expressed in two different ways

$$-k \frac{\partial T}{\partial r_{r=R}} = h_i(T_{\text{vapor}} - T_{\text{wall}}) = \rho_w V h_{fg} \tag{1}$$

where k is the wall's thermal conductivity, T is the temperature in the wall, r is the radial coordinate in the wall, R is the vapor space radius, h_i is an evaporation/condensation coefficient, T_{vapor} is the vapor temperature, T_{wall} is the internal wall surface temperature, ρ_w is the density of vapor leaving the wall, V is the radial velocity at which vapor enters the wall, and h_{fg} is the latent heat of evaporation for the liquid. The first of the two expressions is a boundary condition for the wall heat conduction model. The second expression is a boundary condition for the vapor model. Equation (1) couples the wall model to the vapor model.

In Eq. (1), the evaporation/condensation coefficient h_i is required. For this numerical model, an expression for the molecular flux of evaporation presented by Collier[11] is used. Starting with Collier's relationship and then assuming the vapor is a saturated vapor, Eq. (2) is derived:

$$h_i = 1.01 \times 10^{-15} T_{\text{vapor}}^{7.6} \tag{2}$$

Equation (2) predicts very high values for h_i, which is consistent with the evaporation/condensation process. In Eq. (2), the evaporation/condensation coefficient has units of W/(m²K) while temperature is in degrees K.

The Vapor Model

For the vapor model the flow is assumed to be one-dimensional, compressible in time, incompressible in space, and quasisteady. At the beginning of any time-step, the vapor's density and temperature are known. Because the flow is assumed to be incompressible in space, the density and temperature of the vapor are constant throughout the vapor space. With the knowledge of the vapor's temperature, and the temperature distribution in the heat-pipe wall, Eq. (1) is used to find the distribution of mass evaporation and condensation along the length of the heat-pipe's vapor channel ($\rho_w V(z)$). From the mass evaporation and condensation distribution, conservation of mass is used to find the rate of mass storage in the heat-pipe vapor space

$$\frac{\partial m}{\partial t} = 2\pi R \int_0^L (\rho_w V)\, \mathrm{d}z \tag{3}$$

where m is the mass in the vapor space $m = \pi R^2 L \rho$, L is the length of the vapor space, t is time, and z is the axial coordinate.

With a knowledge of the initial mass in the vapor space and the rate of mass storage from Eq. (3), the mass in the vapor space at a new time-step can be found using the expression below:

$$m^{n+1} = m^n + \Delta t\, (\partial m/\partial t) \tag{4}$$

where m^{n+1} and m^n are the mass in the vapor space at a new and the old time-steps, respectively.

Once the new mass (and, thus, density) is found using Eq. (4), the new vapor temperature is needed to complete marching the solution one time-step through time. The new temperature is found by assuming the vapor to be saturated. For a saturated vapor, the vapor density and temperature are dependent properties. The equation used to relate density and temperature is

$$\rho = 1.07 \times 10^{-42} T^{16.2} \tag{5}$$

Equation (5) was found by curve-fitting steam table saturation vapor data. In Eq. (5) density has units of kg/m³ and temperature has units of degrees Kelvin.

With the knowledge of the new vapor density and temperature, it is possible to continue marching the solution through time. At any time-step during the process, it is possible to determine the axial distribution of velocity and pressure in the heat-pipe vapor space.

The velocity distribution can be found by integrating the one-dimensional, steady, incompressible continuity equation

$$\rho \frac{\partial u}{\partial z} + \frac{2\rho_w V}{R} = 0 \tag{6}$$

where u is the mean axial velocity. The pressure distribution can be found by integrating the one-dimensional, incompressible, steady, axial momentum equation

$$\frac{\partial p}{\partial z} + \rho \frac{\partial u^2}{\partial z} + \frac{2\tau_w}{R} = 0 \tag{7}$$

where p is the change in pressure relative to the saturation pressure corresponding to current saturation conditions, and τ_w is a local shear stress. The shear stress was modeled as

$$\tau_w = f \frac{\rho u^2}{2} \tag{8}$$

where f is a friction coefficient. The friction coefficient f is found using the model developed by Bowman, which takes into account mass evaporation and condensation.[1]

For a region with evaporation, the friction coefficient is found using the relationship

$$f = 16/Re\,(1.2337 - 0.2337 e^{0.0363 Re_w}) e^{6M^{2/5}} \tag{9}$$

where M is the local Mach number based on local mean axial velocity, Re_w is the local radial Reynolds number, and Re is the local axial Reynolds number defined as

$$Re_w = 2\rho_w V R/\mu \tag{10}$$

$$Re = 2\rho u R/\mu \tag{11}$$

where μ is fluid viscosity. For a condensation region

$$f = \frac{0.046}{Re^{1/5}} \left[1 + 55 Re^{0.1} \left(\frac{v_0}{u}\right)^{0.9} \left(\frac{2L_c}{D}\right)^{0.1} e^{6M^{2/5}} \right] \tag{12}$$

where L_c is the length of the mass extraction region. More information on the limitations of Eqs. (9) and (12) can be found in Ref. 1.

One should not be troubled with the contradictory statements, density and temperature are constant; however, pressure varies. As long as the variation in pressure is small, the resulting variations in density and temperature are negligible and can be ignored, while still obtaining good engineering accuracy. This assumption holds for most heat-pipe applications. An exception would be if a heat pipe approaches the sonic limit, where pressure variations would be too large to assume incompressible (constant density and temperature) flow.

The solution process described above has several advantages over solution techniques that have been proposed during the last few years. First, it is not necessary to solve for the vapor velocity or pressure distribution in order to advance the solution through time; however, the velocity and pressure distributions can be found at any time if they are required. This results in a simpler computer model compared to earlier models. The second and more important advantage is related to the assumption of saturated vapor in the vapor space. Earlier models always assumed the vapor to be an ideal gas. It can be shown that saturated vapor thermodynamic properties closely follow ideal gas behavior at low pressures; however, ideal gas behavior does not uniquely define saturated vapor behavior. In other words, assuming the vapor is an ideal gas does not require the vapor to stay close to saturated vapor behavior. Large departures from saturated vapor behavior can lead to predicting artificially high velocities in the heat pipe, which, in turn, leads to overestimating the axial pressure drop in the vapor space. Assuming the vapor is a saturated vapor (and not making the ideal gas assumption) solves this problem.

Two stability constraints exist for the solution procedure. For the explicit solution procedure used to model the transient conduction in the heat-pipe wall, the time-step was limited by the expression[10]

$$\Delta t \leq 2\Delta r^2/\alpha \tag{13}$$

where Δr is the radial grid spacing in the heat-pipe wall, and α is the wall thermal diffusivity. A second stability constraint related to the vapor model described in this paper is

$$\Delta t < \sigma \frac{R h_{fg}(\rho_E - \rho_c)}{h_i(T_E - T_c)} \tag{14}$$

where ρ_E and ρ_c are the vapor density based on the internal evaporator and condenser wall temperatures, respectively, σ is a safety factor, and T_E and T_c are the internal wall temperatures in the evaporator and condenser, respectively. This expression limits the time-step size so that during any time-step, the temperature of the vapor is bounded by the internal evaporator and condenser temperatures. This is consistent with the Second Law of Thermodynamics. In practice, small values for σ are needed to ensure a stable solution.

In the program, the smaller of the two time-steps is used to march the solution through time. At the beginning of a heat-pipe start-up, the limit of Eq. (14) as $T_E - T_c$ approaches zero must be used for the stability constraint.

Numerical Results

Numerical Grid Studies

To quantify the importance of numerical grid on the solution, a grid study was conducted. Figures 1 and 2 represent the results of the study. Three different solutions are shown in Fig. 1 for three different time-step sizes. All three solutions used a 3 × 11 grid (3 nodes radially through the wall, 11

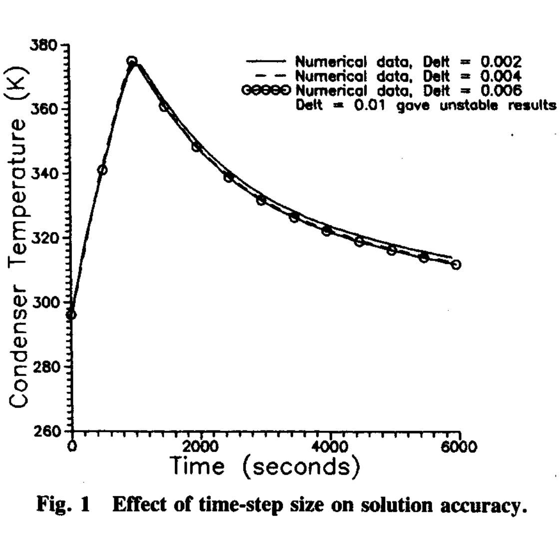

Fig. 1 Effect of time-step size on solution accuracy.

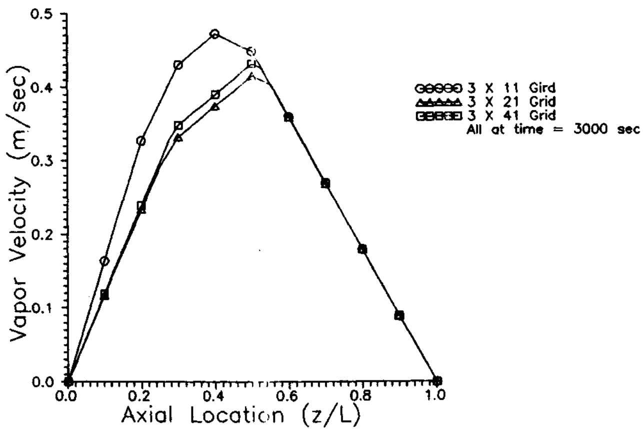

Fig. 2 Effect of axial grid size on solution accuracy.

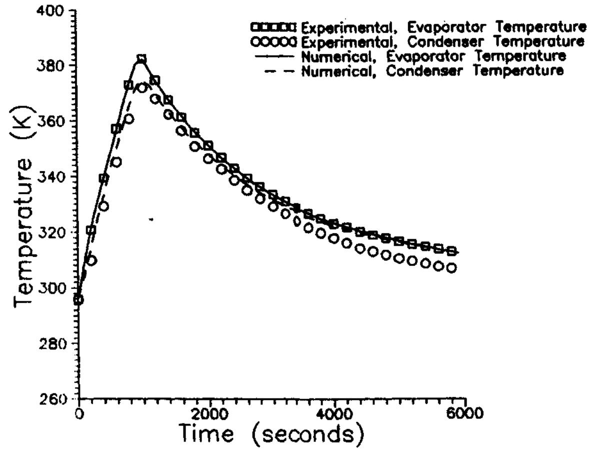

Fig. 3 Comparison of experimental and numerical data for the heat-pipe transient.

nodes axially along the heat-pipe wall and vapor space). When a time-step larger than the three shown in Fig. 1, was tried, an unstable solution resulted. Except for stability considerations, time-step size had a minimum effect on solution accuracy. Figure 2 compares three different spatial grids, 3 × 11, 3 × 21, and 3 × 41. As can be seen from the figure, axial grid resolution leads to a converging velocity solution. When results from two different radial grids, 3 × 41 and 9 × 41, were compared, no difference could be seen in the solutions. A 3 × 41 grid was used for the results presented in the remainder of this paper.

Comparison of Numerical Results with Experimental Data

The heat pipe used to obtain experimental results is 0.61-m long, has an outside diameter of 1.59 cm and a wall thickness of 0.159 cm. The heat-pipe container and wick are copper and it is filled with 14.3 cc of water. The wick consists of four wraps of 100 mesh/in. copper screen. The total wick thickness is 0.1–0.13 cm. The internal dimensions of the heat pipe are estimations based on standard material dimensions. The evaporator section of the heat pipe is 0.18 m long. It is wrapped with an electric heating element and then insulation to ensure most of the energy produced by the heater enters the heat pipe. The heat pipe has an adiabatic section that is 0.16 m long and a 0.34-m condenser. The condenser was cooled by free convection to the air around the heat pipe.

The experimental transient consisted of starting the heat pipe with a step increase in power to the evaporator. After 20 minutes, the heater was turned off and the heat pipe was allowed to cool. Figure 3 compares the numerical obtained results with the copper water heat-pipe experimental data.

The numerical and experimental results show excellent agreement during the first half of the transient. Late in the

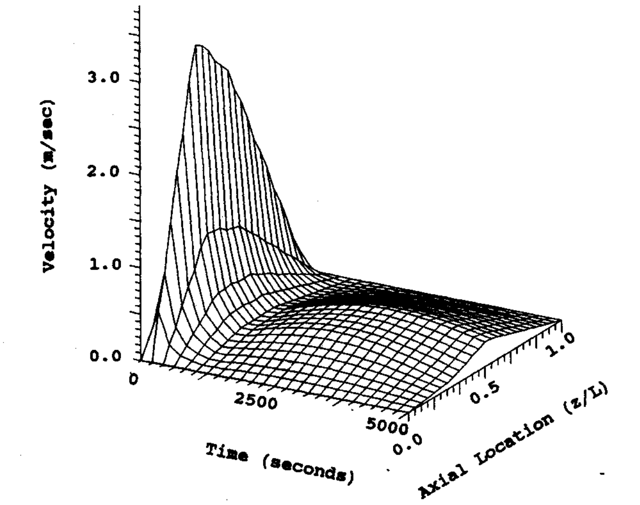

Fig. 4 Vapor velocity as a function of time and location for the heat-pipe transient.

transient, the external condenser temperature is shown to drift higher than the experimental values. This may be a result of incorrectly modeling the convection process from the condenser surface to the environment.

Figure 4 shows how the vapor velocity varies both axially and with time during the transient. The vapor velocities at the ends of the pipe were always 0 m/s as would be expected. It is interesting to note the larger velocities early in the transient. This is a result of the initially small vapor density. As the heat pipe warms up, and the vapor density increases, the vapor velocities decrease. As the heat pipe is cooled (time >1200 s) the velocity is seen to increase and then eventually decrease. Once again, this is a result of vapor density variations combined with the change in power throughput. Figure 4 shows the axial variation in velocity as well. It can be seen that the velocity always increases along the evaporator and decreases along the condenser section of the heat pipe. Along the adiabatic section of the heat pipe, the velocity is seen to decrease while the heat pipe is warming up, and increase while the heat pipe is cooling down. Velocity variations in the adiabatic section are a result of the thermal mass of this part of the heat pipe. It is felt that the model does an excellent job of modeling the heat-pipe vapor flow. The model provides the researcher with more information than can be verified experimentally.

Conclusions

This paper presents a simple way of modeling the transient vapor behavior found in heat pipes. For the model, the vapor is assumed to be quasisteady, compressible in time, incompressible in space, and one-dimensional. The model is shown to do an excellent job of modeling a heat-pipe transient. The model would be excellent for coupling with developmental code for studying more complicated heat-pipe phenomena.

References

[1]Bowman, W. J., *Simulated Heat-Pipe Vapor Dynamics*, Ph.D. Dissertation, Air Force Institute of Technology, Wright-Patterson AFB, Dayton, OH, 1987.

[2]Issacci, F., Ghoniem, N., and Catton, I., "Vapor Flow Patterns During a Startup Transient in Heat Pipes," *AIAA/American Society of Mechanical Engineers Fifth Joint Thermophysics and Heat Transfer Conference*, Seattle, WA, June 18–20, 1990.

[3]Faghri, A., "Transient Heat Pipe Code," Joint NASA/Air Force Transient Heat Pipe Code Workshop, NASA Lewis Research Center, Cleveland, OH, Aug. 6, 1990.

[4]El-Genk, M., "Transient Heat Pipe Code," Joint NASA/Air Force Transient Heat Pipe Code Workshop, NASA Lewis Research Center, Cleveland, OH, Aug. 6, 1990.

[5]Hall, M. L., and Doster, J., "Transient Thermohydraulic Heat Pipe Modeling," *Proceedings of the Fourth Symposium on Space Nuclear Power Systems*, Albuquerque, NM, Jan. 12–16, 1987.

[6]Costello, F., Montague, A., Merrigan, M., and Reid, R., "A Detailed Transient Model of a Liquid-Metal Heat Pipe," *Proceedings of the Fourth Symposium on Space Nuclear Power Systems*, Albuquerque, NM, Jan. 12–16, 1987.

[7]Bowman, W. J., and Sweeten, R. W., "Numerical Heat-Pipe Modeling," *AIAA 24th Thermophysics Conference*, AIAA Paper 89-1705, Buffalo, NY, June 1989.

[8]Chang, M., and Chow, L., "Transient Behavior of Axially Grooved Heat Pipe with Thermal Energy Storage," *AIAA/American Society of Mechanical Engineers Fifth Joint Thermophysics and Heat Transfer Conference*, AIAA Paper 90-1754, Seattle, WA, June 18–20, 1990.

[9]Bowman, W. J., "Numerical Modeling of Heat-Pipe Transient," *Journal of Thermophysics and Heat Transfer*, Vol. 5, No. 3, 1991, pp. 374–379.

[10]Incropera, F. P., and DeWitt, D. P., *Introduction to Heat Transfer*, 2nd ed., Wiley, New York, 1990, pp. 270–273.

[11]Collier, J. G., *Convective Boiling and Condensation*, McGraw-Hill, New York, 1981.

Technical Comments

Comment on "Natural Convection from Isothermal Plates Embedded in Thermally Stratified Porous Media"

Adrian Bejan*
Duke University, Durham, North Carolina 27706

IN their presentation of the history, the authors failed to mention that the first and only time that the problem of natural convection from a vertical surface to a linearly stratified porous medium was treated in the literature was in Ref. 1. This problem is precisely the one for which Lai et al. report concrete results.

It is true that they mentioned my "integral solutions" once, in the tenth to the last line of the paper, but this does not change the impression that is conveyed in their *Introduction* regarding the history of the problem. Furthermore, my work is included in but not credited on their Fig. 2.[2] (see Fig. 1).

I take this opportunity to report an original and much simpler means of estimating the effect of stratification on the total heat transfer rate. To accomplish this, I reproduce the graph in which my 1984 solution is reported. This graph answers the question: given the *maximum* temperature difference $\Delta T = (T_0 - T_{\infty,0})$, the wall height H, and the stratification rate γ (or b, dimensionless, defined on the figure), what is the overall heat transfer rate? In this figure, the overall Nusselt number and the Rayleigh number are based on the maximum temperature difference, namely $Nu_{0-H} = \overline{q''}H/(k\Delta T)$ and $Ra_H = g\beta KH\Delta T/(\alpha\nu)$.

The filled circle drawn for the case of no stratification ($b = 0$) represents Cheng and Minkowycz' exact solution,[3] which

Received May 29, 1991; accepted for publication Oct. 30, 1991.

*J. A. Jones Professor of Mechanical Engineering.